



# The therapeutic effects of resveratrol on hepatic steatosis in high-fat diet-induced obese mice by improving oxidative stress, inflammation and lipid-related gene transcriptional expression

Kang Cheng<sup>1</sup> · Zhihua Song<sup>1,2</sup> · Hao Zhang<sup>1</sup> · Simian Li<sup>1</sup> · Chao Wang<sup>1</sup> · Lili Zhang<sup>1</sup> · Tian Wang<sup>1</sup>

Received: 3 November 2018 / Accepted: 13 January 2019 / Published online: 23 January 2019  
© The Japanese Society for Clinical Molecular Morphology 2019

## Abstract

So far, the majority of the previous animal studies have focused on the preventive effects of resveratrol (RSV) on non-alcoholic fatty liver disease (NAFLD) rather than the therapeutic effects. In this study, the therapeutic effects of RSV on hepatic oxidative stress (OS), inflammation, and lipid metabolism-related gene expression of obese mice induced by a high-fat diet (HFD) were investigated. Male C57BL/6 mice were fed a HFD for 8 weeks to induce obesity-related NAFLD model. And then, NAFLD mice were treated with daily RSV oral gavage at the dose of 100 mg/kg body weight for an additional 4 weeks. HFD-induced the elevation of serum total cholesterol, high-density lipoprotein cholesterol, glucose, insulin, aspartate aminotransferase and alanine aminotransferase levels, and homeostasis model assessment of insulin resistance, hepatic histology changes, the increases in hepatic triglyceride, malondialdehyde and tumor necrosis factor alpha concentrations, as well as the higher mRNA expression of hepatic toll-like receptor 4 and cluster of differentiation 36 in mice, were restored by RSV. The therapeutic effects of RSV against hepatic steatosis of HFD obese mice were attributed to the reduction of OS, inflammation and free fatty acid uptake.

**Keywords** Resveratrol · Hepatic steatosis · Oxidative stress · Inflammation · Lipid metabolism · Obesity

## Introduction

In recent years, the prevalence of obesity has increased substantially and is considered as a major health problem worldwide [1]. Moreover, obesity individuals have a high risk of numerous diseases, such as type 2 diabetes, cardiovascular disease and hypertension, particularly non-alcoholic fatty liver disease (NAFLD) [2]. NAFLD is one of the most common liver diseases that includes hepatic steatosis, steatohepatitis, fibrosis and hepatic cirrhosis characterized by excessive fat accumulation [triglycerides (TG)] in hepatocytes [3]. Augmented lipid accumulation in hepatocytes is the result of an increased free fatty acid input correlated

with its inefficient  $\beta$ -oxidation, esterification, or both [4]. It is widely acknowledged that oxidative stress (OS) and inflammatory response in hepatocyte of obese individuals are involved in liver lipid accumulation, consequently progressing to hepatic steatosis in the course of NAFLD [4]. Epidemiological and animal studies have demonstrated that the increased reactive oxygen species (ROS) production [5], lower antioxidant levels [5], higher pro-inflammatory cytokines concentrations [6] and aberrant lipid metabolism [7, 8] were observed in the subjects with NAFLD. In addition, a previous study has shown that a pathogenic loop is suggested to link lipid accumulation, inflammation and OS in the liver of obese individuals [9]. Thus, one or several targeted regulations of hepatic lipid metabolism, inflammation and OS may have certain therapeutic effects on NAFLD associated with obesity.

Resveratrol (RSV, 3,5,4'-trihydroxystilbene) is a natural polyphenol that could be found in many plants such as grapes, berries, and peanuts [10]. Accumulating evidence indicates that RSV exhibits anti-cancer, cardio-protective, anti-aging, anti-inflammatory and antioxidant properties [11–14]. Numerous animal studies of RSV on NAFLD have

✉ Tian Wang  
tianwangnjau@163.com

<sup>1</sup> College of Animal Science and Technology, Nanjing Agricultural University, No. 1 Weigang, Nanjing 210095, China

<sup>2</sup> School of electrical and Electronic Engineering, Anhui Science and Technology University, No. 1501 Mount Huangshan Avenue, Bengbu 233100, China

been carried out, and span a wide range of model including rodents and swine, intervention periods and RSV doses [15]. These studies almost uniformly support the beneficial effects of RSV on NAFLD subjects by the inhibition of hepatic de novo lipogenesis and inflammation [11, 16], an increase in fatty acid  $\beta$ -oxidation [17] and the reduction of OS [18]. However, the RSV treatment in the previous experimental documents is generally started from the beginning of the study and, therefore, most of the studies concentrate on the preventive effects of RSV and not the therapeutic effect [15]. It has been hypothesized that whether the therapeutic effects of RSV against the NAFLD are the same as that of RSV in preventive studies. Therefore, in the present study, we investigated the therapeutic effects of RSV on hepatic lipid metabolism, inflammation and OS of obese mice induced by a high-fat diet (HFD). The current study is the first to demonstrate that the hepatic lipid accumulation in obese mice was found to be decreased by RSV through the inhibition of cluster of differentiation 36 (CD36), which may contribute to the suppression of OS and inflammation. Additionally, clinical studies that have been conducted to explore the effects of RSV on hepatic steatosis are scarce. This study may guide the new nutritional intervention for NAFLD patients to alleviate steatosis in clinical setting.

## Materials and methods

### Animal treatment

All experimental procedures on animals were allowed by the Animal Experimental Ethical Committee of Nanjing Agricultural University. Approximately 6-week-old male C57BL/6 mice (19–21 g) were purchased from the Animal Multiplication Centre of Qinglong Mountain (Nanjing, China) and housed in individual cages. During the experimental period, the animals were provided food and water ad libitum, and maintained on a 12-h light/dark cycle in a controlled environment (temperature 20–24 °C; humidity 40–60%). The HFD-NAFLD mice model was established according to the method described previously with some modifications [19, 20]. Briefly, after 1 week of adaptation, mice were randomly allocated to 2 treatments, and fed with a normal control diet (CON group,  $n = 10$ ; #TP23302, fat 10%, carbohydrate 71.0%, protein 19.0%) and a HFD (HFD group,  $n = 20$ ; #TP23300, fat 60%, carbohydrate 20.6%, protein 19.4%) for 8 weeks, respectively. All types of diet were purchased from Trophic Animal Feed High-tech Co Ltd. (Nantong, China). After 8-week induction of NAFLD, HFD group was further divided into 2 subgroups, and oral-fed with 100 mg RSV/kg body weight/day (HFD-RSV group,  $n = 10$ ; 99%, TCI Co., Ltd., Tokyo, Japan) or equivalent volume of 0.5% carboxymethylcellulose sodium

(HFD control group,  $n = 10$ ) for another 4 weeks, while CON group orally received daily vehicle. The administration of RSV dose was based on previous document [21]. From 1 to 12 weeks of this experiment, mice were continued on their original diets, and inspected daily for food intake and weighted weekly. At the end of the experiment, mice were anesthetized with phenobarbital sodium (50 mg/kg) following a 12-h fast and blood was taken from the eye enucleation to measure serum biomarkers. After that, the liver and white adipose tissues (epididymal and perirenal adipose tissue) were quickly removed, rinsed with physiological saline, blotted and weighed. Among them, one part of the liver was stored in liquid nitrogen until used for lipid measurement, enzyme activity and/or RNA analysis, and the other part of liver tissue was fixed in 4% paraformaldehyde for histology.

### Serum biochemical parameters

The glucose, TG, total cholesterol (TC), high-density lipoprotein cholesterol (HDL-C), and low-density lipoprotein cholesterol (LDL-C) levels in the serum were measured using commercial kits (Shanghai Kehua Bio-Engineering co., Ltd., Shanghai, China) with automatic biochemical analyzer (Selecta E, Wasson, Eindhoven, Holland). The commercial kits (Nanjing Jiancheng Institute of Bioengineering, Nanjing, China) were used to analyse the serum alanine aminotransferase (ALT) and aspartate aminotransferase (AST) activities. The serum insulin level was estimated using a commercial enzyme-linked immunosorbent assay (ELISA) kit (Elabscience Biotechnology Co., Ltd., Wuhan, China) according to the manufacturer's instructions. The detection limits were for 0.31 ng/mL insulin; the inter- and intra-assay coefficients were < 10%. The homeostasis model assessment of insulin resistance (HOMA-IR) was used to calculate the insulin resistance according to the following formula [22]:  $\text{HOMA-IR} = \text{fasting serum insulin } (\mu\text{U/mL}) \times \text{fasting plasma glucose (mmol/L)} / 22.5$ .

### Histology of liver

After being dehydrated with graded alcohol series, liver samples were embedded in paraffin and cut into sections. Sections with 5  $\mu\text{m}$  thickness were stained with hematoxylin and eosin (HE). For hepatic lipid staining, frozen liver tissues were cryosectioned, briefly fixed in 10% formalin, and stained with Oil Red O.

### Hepatic TG analysis

The hepatic lipids were extracted with a chloroform/methanol (2:1, v/v) solution by the method of Folch et al. [23]. According to the instructions of the manufacturer, the hepatic TG level was measured using commercially

available kits (Nanjing Jiancheng Institute of Bioengineering, Nanjing, China).

### Liver homogenate preparation

Approximately 0.5 g of liver sample was diluted 1:4 (w/v) with ice-cold 0.9% sodium chloride buffer and homogenized by Ultra-Turrax homogenizer (Tekmar Co., Cincinnati, OH), and centrifuged at 4550g for 15 min at 4 °C. The supernatant was collected and rapidly stored in –20 °C until the subsequent analysis. The protein concentration in the homogenate was determined by the Bradford method [24].

### Analysis of hepatic OS

The activities of hepatic total superoxide dismutase (T-SOD) and glutathione peroxidase (GPX), the glutathione (GSH) level and the concentration of malondialdehyde (MDA) were determined using commercially available assay kits (Nanjing Jiancheng Institute of Bioengineering, Nanjing, China), in line with the manufacturer's instructions [25]. All results were normalized to total protein concentration in each sample for inter-sample comparison.

### Determination of hepatic cytokines

Liver concentrations of tumor necrosis factor alpha (TNF- $\alpha$ ) and interleukin 6 (IL-6) were measured by commercial ELISA kits (Elabscience Biotechnology Co., Ltd., Wuhan, China) following the manufacturer's protocols. The minimum detectable concentrations of TNF- $\alpha$  and IL-6 were 31.25 pg/mL and 31.25 pg/mL, respectively. The intra- and inter-assay coefficients of variation were <10% and <10% for TNF- $\alpha$ , <10% and <10% for IL6, respectively.

### Total RNA isolation and mRNA quantification

The mRNA abundance was performed as previously described [26]. Total RNA was isolated from snap-frozen liver samples using TRIzol Reagent (TaKaRa Biotechnology, Dalian, China). The 1% agarose gel with ethidium bromide staining was used to confirm the integrity of the samples. After the determination of RNA concentration, 1  $\mu$ g of total RNA was reverse-transcribed into complementary DNA using the PrimeScript RT Reagent Kit (TaKaRa Biotechnology, Dalian, China) according to the manufacturer's protocol. Real-time PCR was carried out on an ABI StepOnePlus Real-Time PCR system (Applied Biosystems, Foster City, CA, USA) according to the manufacturer's instructions. The primer sequences of the target and reference genes (SOD, GPX, TNF- $\alpha$ , IL-6, toll-like receptor 4 (TLR4), cluster of differentiation 68 (CD68), adhesion G protein-coupled receptor E1 (F4/80), CD36, microsomal

triglyceride transfer protein (MTP), sterol regulatory element-binding protein 1c (SREBP-1c), fatty acid synthase (FAS), acetyl-CoA carboxylase (ACC), stearyl-CoA desaturase-1 (SCD-1), peroxisome proliferator-activated receptor alpha (PPAR- $\alpha$ ), PPAR- $\gamma$ , carnitine palmitoyltransferase 1 alpha (CPT-1 $\alpha$ ) and  $\beta$ -actin) used in real-time PCR are given in Table 1. Briefly, the reaction mixture was prepared using 2  $\mu$ L of complementary DNA, 0.4  $\mu$ L of forward primer, 0.4  $\mu$ L of reverse primer, 10  $\mu$ L of SYBR Premix Ex Taq (TaKaRa Biotechnology, Dalian, China), 0.4  $\mu$ L of ROX Reference Dye (TaKaRa Biotechnology, Dalian, China), and 6.8  $\mu$ L of double-distilled water. Each sample was tested in duplicate. PCR consisted of a pre-run at 95 °C for 30 s and 40 cycles of denaturation at 95 °C for 5 s, followed by a 60 °C annealing step for 30 s. The conditions of the melting curve analysis were as follows: one cycle of denaturation at 95 °C for 10 s, followed by an increase in temperature from 65 to 95 °C at a rate of 0.5 °C/s. The relative levels of mRNA expression were calculated using the  $2^{-\Delta\Delta C_t}$  method [27] after normalization to those of  $\beta$ -actin as a housekeeping gene. The values of CON group were used as a calibrator.

### Statistical analysis

All data were analyzed by one-way ANOVA using the SPSS 16.0 (SPSS Inc., Chicago, IL). Tukey's multiple range test was used to compare the differences among groups. All data are expressed as mean  $\pm$  SE. The level of statistical significance was considered to be  $P < 0.05$ .

## Results

### Body weight, food intake and organ weight

During 1–8 weeks, the body weight of HFD mice was higher ( $P < 0.05$ ) than that of CON mice (Fig. 1b). The body weight was also significantly elevated ( $P < 0.05$ ) in the HFD mice relative to the CON group from week 9 to week 12 (Fig. 1d), while the RSV treatment did not affect the body weight ( $P > 0.05$ ). Meantime, the food intake was not significantly altered ( $P > 0.05$ ) by RSV and HFD through the whole experiment (Fig. 1a, c). At week 12, the organ weight (liver, epididymal and perirenal white adipose tissue) was greater ( $P < 0.05$ ) in the HFD mice compared to the CON mice (Fig. 1e, f). Unfortunately, RSV had no effect on the organ weight in the HFD-RSV mice compared to the HFD mice ( $P > 0.05$ ).

### Serum metabolic parameters

At week 12, HFD increased ( $P < 0.05$ ) the serum TG, TC, glucose, HDL-C, LDL-C, insulin and HOMA-IR levels

**Table 1** Sequences for real-time PCR primers

Gene	Forward primer (5'→3')	Reverse primer (5'→3')
SOD	CAGACCTGCCTTACGACTATGG	CTCGGTGGCGTTGAGATTGTT
GPX	AGTCCACCGTGTATGCCTTCT	GAGACGCGACATTCTCAATGA
TNF- $\alpha$	GGCAGGTCTACTTTGGAGTCATTGC	ACATTCGAGGCTCCAGTGAATTCGG
IL-6	AGTTGCCTTCTTGGGACTGA	CCACGATTTCCCAGAGAAC
TLR4	TCAGAGCCGTTGGTGTATCTT	CCTCAGCAGGGACTTCTCAA
CD68	TGTCTGATCTTGCTAGGACCG	GAGAGTAACGGCCTTTTTGTGA
F4/80	GAGTGGAATGTCAAGATGTTA	CAGTGAAGAAGAGAAAGC
PPAR- $\gamma$	CACAATGCCATCAGGTTTGG	GCTGGTGCATATCACTGGAGATC
CD36	CTTACACATACAGAGTTCGTTATC	TCCAACAGACAGTGAAGG
MTP	CCGCTGTGCTTGCAAGAAGA	TTTGACACTATTTTTCTGCTATGGT
SREBP-1c	CATGCCATGGGCAAGTACAC	TGTTGCCATGGAGATAGCATCT
FAS	CCCGGAGTCGCTTGAGTATATT	GGACCGAGTAATGCCATTACG
ACC	GTCCCGGCCACATAACTGAT	CGCTCAGGTCACCAAAAAGAAT
SCD-1	CAGTGCCGCGCATCTCT	CCCGGATTGAATCTTCTTG
PPAR- $\alpha$	CGGCAGTGGCCTGAACA	TGGTACCCTGAGGCCTTGTC
CPT-1 $\alpha$	GAACCCCAACATCCCCAAAC	TCCTGGCATTCTCTGGAAT
$\beta$ -actin	CATCCGTAAGACCTCTATGCCAAC	ATGGAGCCACCGATCCACA

SOD superoxide dismutase, GPX glutathione peroxidase, TNF- $\alpha$  tumor necrosis factor alpha, IL-6 interleukin 6, TLR4 toll-like receptor 4, CD68 cluster of differentiation 68, F4/80 adhesion G protein-coupled receptor E1, PPAR- $\gamma$  peroxisome proliferator-activated receptor gamma, CD36 cluster of differentiation 36, MTP microsomal triglyceride transfer protein, SREBP-1c sterol regulatory element-binding protein 1c, FAS fatty acid synthase, ACC acetyl-CoA carboxylase, SCD-1 stearoyl-CoA desaturase-1, PPAR- $\alpha$  peroxisome proliferator-activated receptor alpha, CPT-1 $\alpha$  carnitine palmitoyltransferase 1 alpha,  $\beta$ -actin beta-actin

compared with the control diet (Table 2). The administration of RSV to HFD mice led to decreases ( $P < 0.05$ ) in the serum levels of TC, HDL-C, glucose, insulin and HOMA-IR.

### Hepatic morphology, function, Oil Red staining, and TG level

As shown in Fig. 2a, the CON mice displayed normal liver histology. However, the HFD mice exhibited classical steatosis such as ballooning degeneration and inflammatory foci compared with that of the normal control mice. Additionally, hepatic injury index (serum AST and ALT levels) was higher in the HFD mice (Fig. 2c). Furthermore, hepatic TG content was higher in HFD-fed mice than that in CON mice (Fig. 2c). The Oil Red staining results further validated that HFD induced hepatic lipid deposition (Fig. 2b). As expected, RSV treatment attenuated the elevation of hepatic TG, serum AST and ALT contents, and the changes of pathology in the HFD mice.

### Hepatic redox status

The hepatic MDA (Fig. 3c) concentration was higher ( $P < 0.05$ ) in the HFD group compared with the CON group. As expected, the RSV treatment in the HFD-RSV restored ( $P < 0.05$ ) the increased MDA content and elevated T-SOD ( $P < 0.05$ , Fig. 3a) and GPX ( $P = 0.099$ , Fig. 3b) activities

in the liver compared with the HFD group. In addition, the changes of SOD (Fig. 3d) gene transcriptional expression were similar with that of its activities. No differences were observed in hepatic GSH level and GPX gene expression among treatments ( $P > 0.05$ , Fig. 3e, f).

### Hepatic inflammation

The increased ( $P < 0.05$ ) TLR4 mRNA expression and TNF- $\alpha$  concentration were found in the liver of the HFD group compared with the CON group (Fig. 4a, b). Compared with the HFD group, the protein and mRNA abundance of TNF- $\alpha$  and TLR4 gene expression were significantly reduced ( $P < 0.05$ ) in the HFD-RSV group due to the RSV treatment. No differences ( $P > 0.05$ ) were noted between the groups with regard to the IL-6 protein and gene expression, F4/80 and CD68 gene expression levels in the liver.

### Hepatic expression of genes involved in lipid metabolism

Compared with the CON mice, the HFD mice had the increased ( $P < 0.05$ ) CD36 and PPAR- $\gamma$  mRNA abundance in the liver (Fig. 5). RSV administration decreased ( $P < 0.05$ ) hepatic CD36 mRNA expression level in the HFD-RSV group when compared with the HFD group. There were no statistically significant differences in SREBP-1c, FAS, ACC,

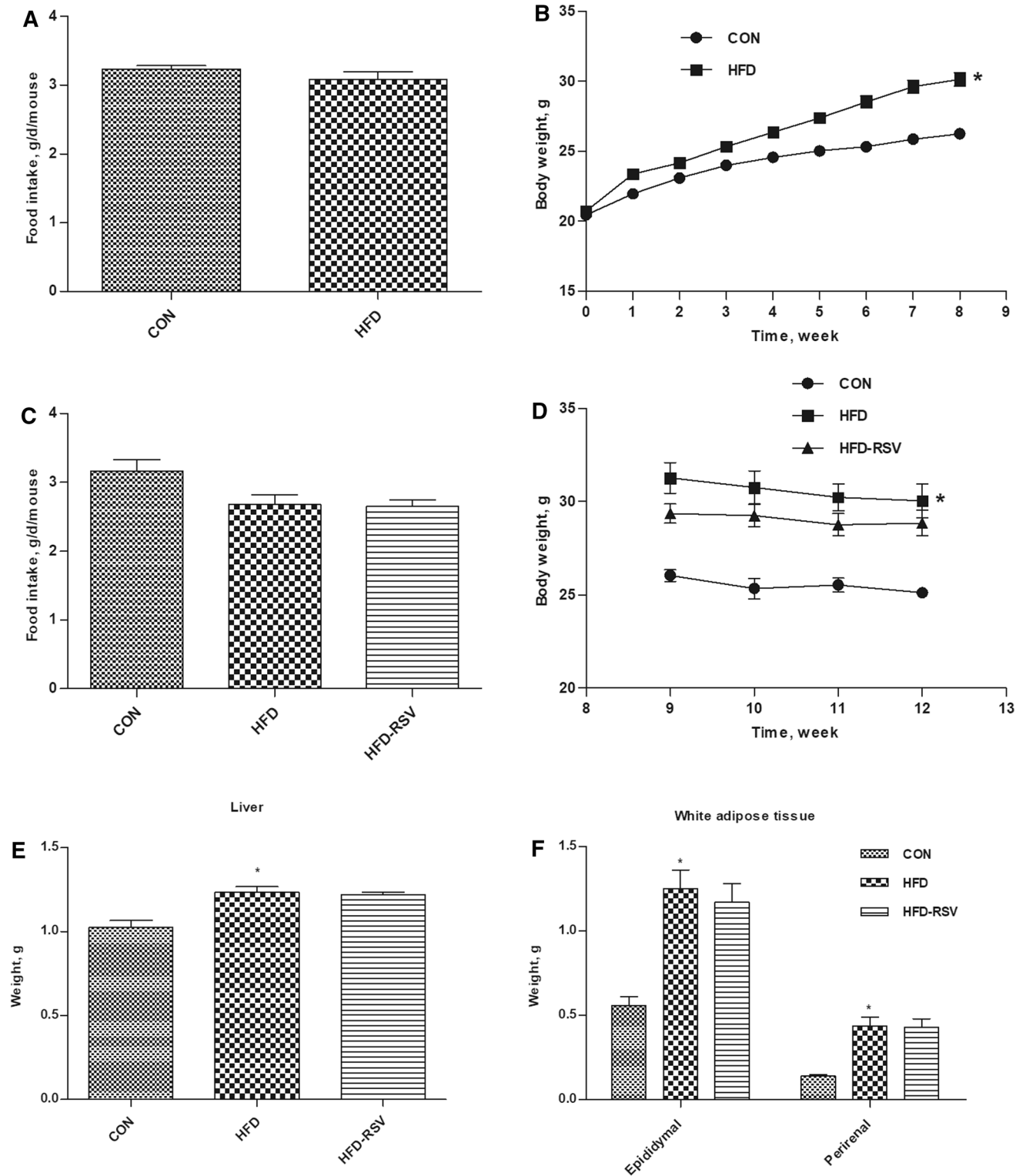


**Fig. 1** Body weight, food intake and organ weight of mice. **a** Food intake and **b** body weight in mice fed HFD (CON,  $n=10$ ; HFD,  $n=20$ ) during 1–8 weeks. **c** Food intake and **d** body weight during 9–12 weeks after administration of resveratrol to HFD mice ( $n=10$ ). **e** Liver weight and **f** epididymal and perirenal white adipose tissue

weight in mice at 12 weeks ( $n=10$ ). CON control diet, HFD high-fat diet, HFD-RSV high-fat diet plus resveratrol treatment. Data are expressed as the mean  $\pm$  SE. \* $P < 0.05$  when compared with the CON group

**Table 2** Serum parameters in mice

Items	CON	HFD	HFD-RSV
TG, mmol/L	0.15 ± 0.04	0.93 ± 0.28*	0.60 ± 0.14
TC, mmol/L	0.57 ± 0.29	3.92 ± 0.24*	1.26 ± 0.36 <sup>#</sup>
HDL-C, mmol/L	0.30 ± 0.07	2.22 ± 0.10*	0.42 ± 0.13 <sup>#</sup>
LDL-C, mmol/L	0.18 ± 0.04	0.37 ± 0.05*	0.22 ± 0.03
Glucose, mmol/L	6.28 ± 2.67	34.21 ± 4.65*	11.00 ± 3.34 <sup>#</sup>
Insulin, μU/mL	11.24 ± 5.54	29.14 ± 2.54*	14.94 ± 1.38 <sup>#</sup>
HOMA-IR	6.40 ± 5.06	45.87 ± 8.82*	7.19 ± 2.39 <sup>#</sup>

Data are expressed as the mean ± SE ( $n = 10$ ). \* $P < 0.05$  when compared with CON group, <sup>#</sup> $P < 0.05$  when compared with HFD group

CON control diet, HFD high-fat diet, HFD-RSV high-fat diet plus resveratrol treatment, TG triglyceride, TC total cholesterol, HDL-C high-density lipoprotein cholesterol, LDL-C low-density lipoprotein cholesterol, HOMA-IR homeostasis model assessment-insulin resistance

SCD-1, PPAR- $\alpha$ , CPT-1 $\alpha$ , MTP mRNA expression levels

between the groups ( $P > 0.05$ ).

## Discussion

Many lines of evidence regarding RSV have focused on the protective or beneficial effects on NAFLD or non-alcoholic steatohepatitis (NASH) [4, 11, 19]; limited studies have been performed to elaborate RSV-mediated therapeutic role against established NAFLD injury. In the current study, to establish obesity-related NAFLD model, the mice were fed a HFD for 8 weeks and it was observed that mice developed heavier body weight, higher hepatic injury makers (serum AST and ALT levels) and glucose metabolism disorder (higher serum glucose and insulin level, HOMA-IR), implying the successful development of NAFLD in this model (unpublished data). These results are in agreement with previous studies that showed the development of NAFLD by a

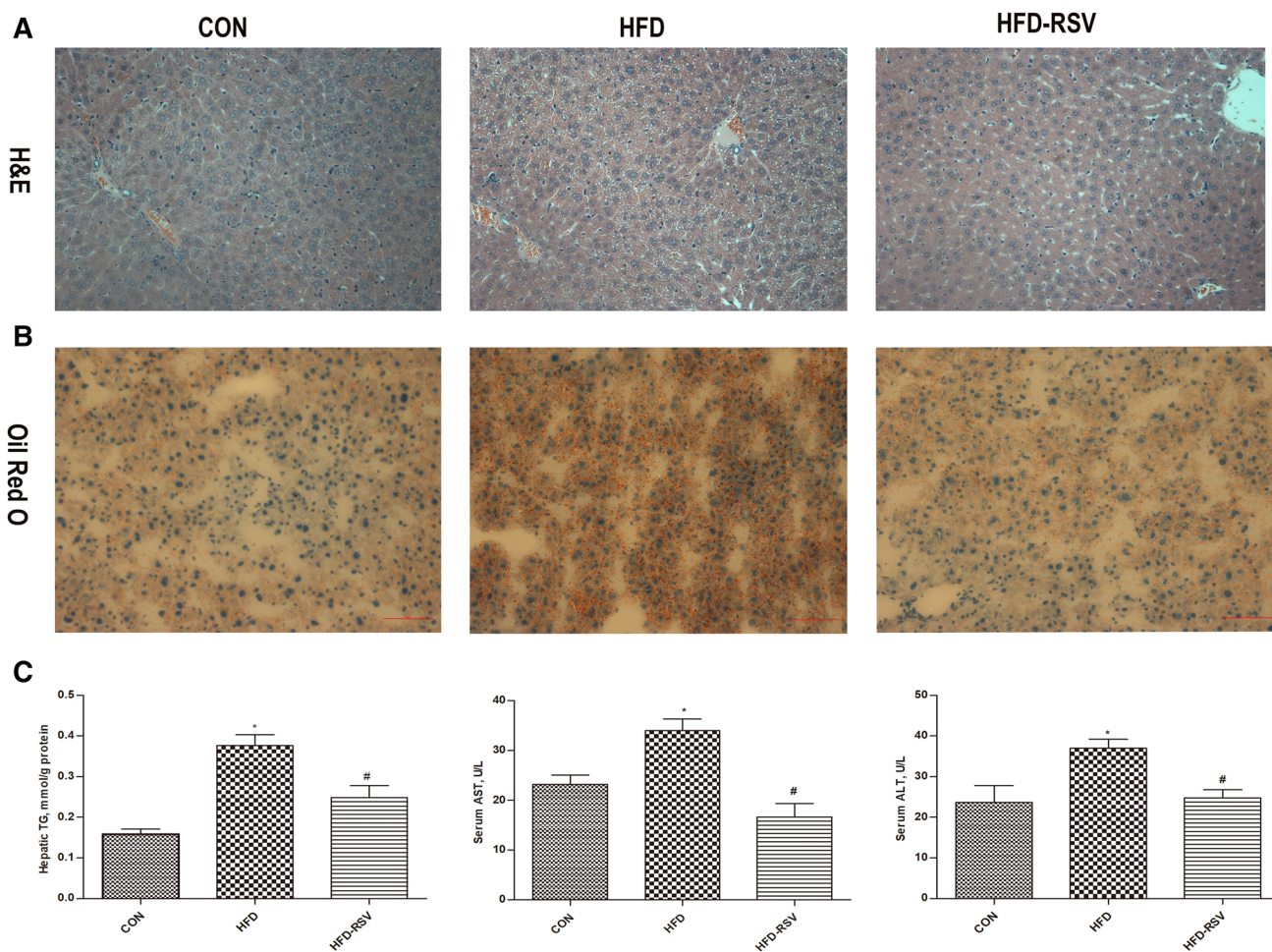


**Fig. 2** Hepatic morphology, function and lipid deposition in mice. **a** Hematoxylin and eosin (H&E) and **b** Oil Red O staining of representative liver sections (magnification,  $\times 200$ ). **c** Hepatic triglyceride (TG), serum aspartate aminotransferase (AST) and alanine ami-

notransferase (ALT) levels. CON control diet, HFD high-fat diet, HFD-RSV high-fat diet plus resveratrol treatment. Data are expressed as the mean ± SE ( $n = 10$ ). \* $P < 0.05$  when compared with the CON group, <sup>#</sup> $P < 0.05$  when compared with the HFD group

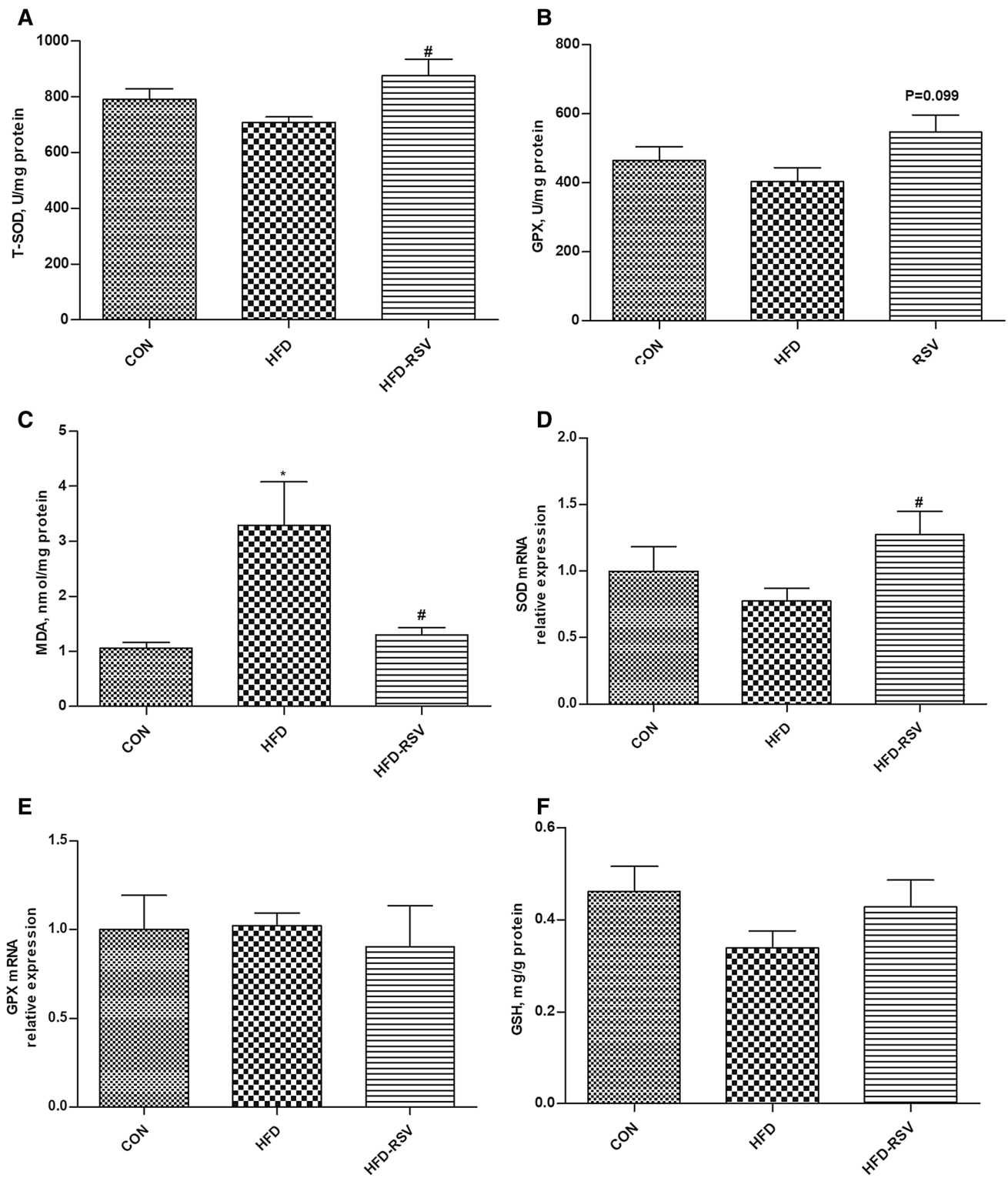


**Fig. 3** Hepatic redox status in mice. **a** Total superoxide dismutase (T-SOD) activity. **b** Glutathione peroxidase (GPX) activity. **c** Malondialdehyde (MDA) concentration. **d** SOD mRNA relative expression. **e** GPX mRNA relative expression. **f** Glutathione (GSH) level.

CON control diet, HFD high-fat diet, HFD-RSV high-fat diet plus resveratrol treatment. Data are expressed as the mean ± SE (n = 10). \*P < 0.05 when compared with the CON group, #P < 0.05 when compared with the HFD group

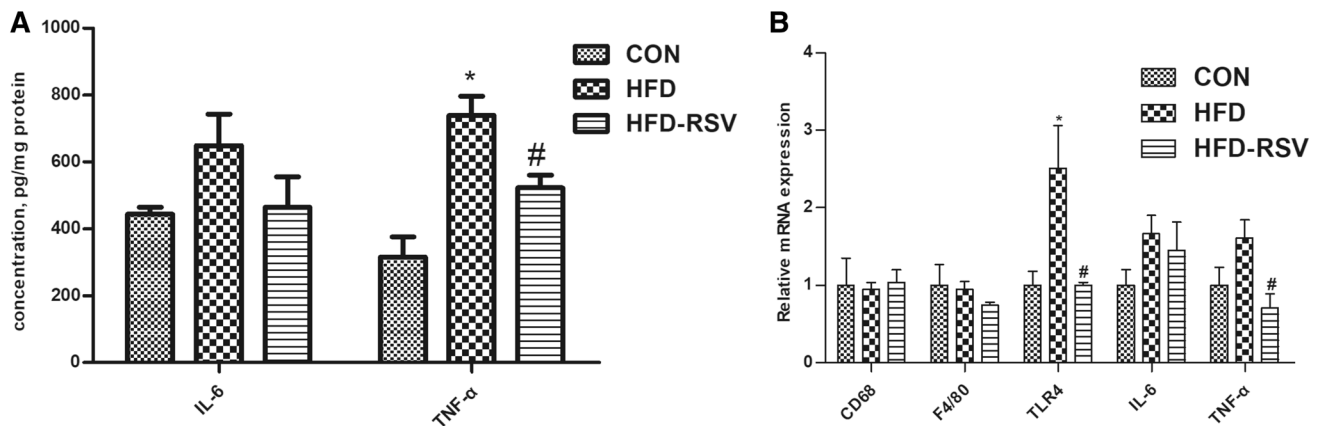


**Fig. 4** Hepatic inflammatory response in mice. **a** The interleukin 6 (IL-6) and tumor necrosis factor alpha (TNF- $\alpha$ ) concentrations. **b** The inflammation-related gene expression. CON control diet, HFD high-fat diet, HFD-RSV high-fat diet plus resveratrol treatment, TLR4 toll-

like receptor 4, CD68 cluster of differentiation 68, F4/80 adhesion G protein-coupled receptor E1. Data are expressed as the mean  $\pm$  SE ( $n=10$ ). \* $P<0.05$  when compared with the CON group, # $P<0.05$  when compared with the HFD group

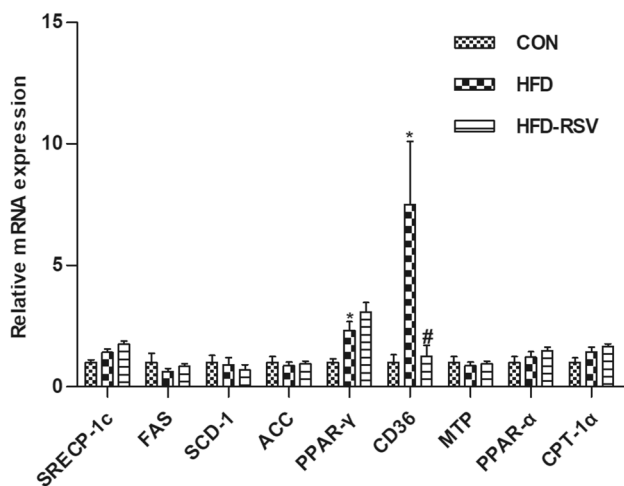


**Fig. 5** Hepatic lipid metabolism-related gene expression in mice. CON control diet, HFD high-fat diet, HFD-RSV high-fat diet plus resveratrol treatment, SREBP-1c sterol regulatory element-binding protein 1c, FAS fatty acid synthase, SCD-1 stearoyl-CoA desaturase-1, ACC acetyl-CoA carboxylase, PPAR- $\gamma$  peroxisome proliferator-activated receptor gamma, CD36 cluster of differentiation 36, MTP microsomal triglyceride transfer protein, PPAR- $\alpha$  peroxisome proliferator-activated receptor alpha, CPT-1 $\alpha$  carnitine palmitoyl transferase 1 alpha. Data are expressed as the mean  $\pm$  SE ( $n=10$ ). \* $P<0.05$  when compared with the CON group, # $P<0.05$  when compared with the HFD group

HFD [19, 20]. In the present study, administration of RSV to HFD obese mice for 4 weeks showed beneficial therapeutic effects in hepatic steatosis, as evidenced by the improvement of glycolipid metabolic parameters, hepatic histology, oxidative status, inflammation and lipid contents. RSV exerted several actions that may contribute to the beneficial effects, including increases in T-SOD and GPX activities, inhibition of TNF- $\alpha$  production as well as suppression expression of

TLR4 and CD 36 at the transcriptional level. Although the conclusions are based on nutritional intervention in HFD mice, the parallel progression of metabolic disease between human and mice suggests the relevance of the present study in the context of nutritional intervention in obese human with NAFLD.

In general, it is accepted that OS is considered to be an important factor in the pathogenesis of NAFLD. OS is an imbalance in favor of the factors that generate ROS and away from the factors that protect cellular macromolecules from these reactants including antioxidants (e.g., SOD and GPX) [28]. The increasing ROS production damages lipid, protein and DNA because of the limited antioxidants. Epidemiological data showed that the higher ROS levels and impaired antioxidant defense systems were observed in patients with NAFLD [29]. Numerous animal studies also reported that the consumption of HFD caused abnormal mitochondrial oxidative phosphorylation and accumulation of ROS [5, 6]. In the present study, MDA, an end product of lipid peroxidation, was increased in the liver of HFD mice, which is in agreement with the study conducted by Li et al. [20]. MDA is commonly used as a reliable biomarker of OS. The results of this study suggested that OS had occurred in the HFD mice. As expected, RSV administration decreased the hepatic MDA contents in HFD-RSV group, which may be explained by the increased T-SOD and GPX activities. SOD catalyzes the reduction of the superoxide anion to hydrogen peroxide, which is degraded into molecular oxygen and water by GPX. Similar observations were noted in the previous study [20]. In a recent study, the therapeutic effects of RSV on renal oxidative damage have been demonstrated in HFD rats, as indicated by the decreased MDA level and increased T-SOD activity [30]. Although RSV can directly scavenge ROS due to the

presence of phenolic hydroxyl groups, its low bioavailability makes it unlikely that the cytoprotective effect can be achieved directly through chemical reactions. A more plausible speculation is that RSV initiates a series of intracellular events that result in the up-regulation of cellular defense systems or inhibition of ROS production, which in turn averts oxidative damage [31]. The mRNA abundance of SOD was up-regulated by RSV in the liver of HFD mice, which may provide an explanation for the increased protein expression of hepatic SOD. The antioxidant property of RSV *in vivo* could be achieved by complexed various molecular mechanism [32]. How RSV could influence diverse signaling pathways in liver of NAFLD subjects, resulting in cellular defense systems activation, should be further investigated in our models.

Obesity associated with HFD also leads to a pronounced increase in recruited hepatic macrophage infiltration in parallel with the local production of inflammatory chemokines and cytokines that are implicated as contributors to hepatic steatosis [16]. In the present study, HFD had no effect on the hepatic F4/80 and CD68 gene expression, which are biomarkers of macrophage infiltration, suggesting that hepatic macrophage infiltration has not happened in the HFD mice. However, the higher hepatic TNF- $\alpha$  profile was still found in the HFD mice in the present study. This could be ascribed to the increased TLR4 mRNA expression. The TLR4 is a member of toll-like receptor which can be indirectly bound and triggered by free fatty acids, resulting in NF-KB activation [33]. Once activated, these pathways can enhance the synthesis and secretion of pro-inflammatory cytokines such as TNF- $\alpha$  from hepatocytes, leading to inflammation. These results of the present study suggested that HFD led to hepatic inflammation in mice due to the local production of cytokines. Interestingly, in the present study, RSV treatment alleviated the hepatic inflammation in the HFD-RSV group evidenced by the down-regulation of TLR4 mRNA expression and TNF- $\alpha$  protein and gene expression levels. The results are consistent with the report of Li et al. [20], who revealed the beneficial and therapeutic effects of RSV on NAFLD pathogenesis in a murine model partially due to the suppression of inflammation via mediating IKB $\alpha$ -NF-KB pathways. Similarly, Jiang et al. [33] reported that oral administration of RSV might be a promising therapeutic treatment for obesity-related osteoarthritis due to the fact that it decreased systematic inflammation levels and/or inhibited TLR4 signaling pathway in cartilage of HFD mice. Pan et al. [30] also suggested that the therapeutic effect of RSV on renal injury in rats fed a HFD partly could be attributed to the suppression of inflammation. It is worthy to state that a vicious cycle among OS and inflammation is observed, and contributes to hepatic steatosis. Therefore, the antioxidant ability of RSV may be beneficial for alleviating hepatic inflammation.

Hepatic lipid accumulation arises when the balance between lipid availability (from circulating lipid uptake or *de novo* lipogenesis) and lipid disposal (via fatty acid oxidation or triglyceride-rich lipoprotein secretion) is disturbed [8]. Unfortunately, aberrant lipid metabolism eventually triggers lipoperoxidative stress, and leads to hepatic injury. In the present study, the higher TG concentration was observed in the liver of HFD mice, which also received the support of the Oil Red O staining results. However, in the current study, no differences were found in various hepatic genes' expression (e.g.,  $\beta$ -oxidation, *de novo* fatty acid synthesis and triglyceride secretion), indicating that lipid disposal and fatty acid biosynthesis were unaltered. At transcriptional level, the hepatic PPAR- $\gamma$  and CD36 were up-regulated in mice by a HFD. When it is overexpressed, hepatic PPAR- $\gamma$  in HFD mice promotes lipid uptake and lipid droplet formation and accelerates the development of steatosis [34]. Previous studies have reported that PPAR- $\gamma$  in the liver was significantly elevated in HFD-NAFLD [16, 35]. As a downstream target of PPAR- $\gamma$ , CD36 mediates fatty acid uptake into cells used for TG synthesis [8]. Previous findings also suggest that increased hepatic CD36 activity may be a critical determinant for the development of steatosis under pathological conditions (e.g., a HFD and obesity) [36, 37]. In contrast, using a deletion method to inhibit the activity of CD36 can delay the development of hepatic steatosis [38]. Clinical study in patients with NAFLD also found that the increased hepatic CD36 gene expression was correlated with liver fat content [39]. Therefore, in the present study, HFD induced abnormal hepatic lipid accumulation via up-regulation of hepatic PPAR- $\gamma$  and its target gene CD36, contributing to hepatic steatosis. To the best of our knowledge, this is the first study to prove that RSV administration alleviated the hepatic lipid accumulation by decreasing the CD36 mRNA expression in the liver of HFD-RSV mice. However, no difference in the PPAR- $\gamma$  mRNA expression was detected in the liver of HFD-RSV mice compared with the HFD mice. These results indicated that RSV improved the hepatic lipid uptake independent of PPAR- $\gamma$ -dependent pathway. In addition to the PPAR- $\gamma$ , the molecular mediators of CD36 transporter expression includes the activation of pregnane X receptor and liver X receptor [8]. This is the first study to explore the therapeutic effects of RSV on the hepatic lipid metabolism in HFD mice. Certainly, more detailed studies in the future are required to explore the molecular mechanisms involved. On the other hand, the improvement of lipid metabolism in the liver of the HFD-RSV mice also has major implications for attenuating OS and inflammation.

## Conclusions

The therapeutic effects of RSV on hepatic steatosis in HFD mice could be achieved through reducing OS, inflammation and fatty acid uptake. This study may provide insights into the role of RSV in treating obese patients with NAFLD.

**Acknowledgements** This work was supported by the National Natural Science Foundation of China (Grant nos. 31772634, 31802094 and 31601948), the National Key Research and Development Program of China (Grant no. 2018YFD0501101), the Postdoctoral Research Foundation of China (Grant no. 2018M632320), the Natural Science Foundation of Jiangsu Province (Grant no. BK20180531), and the Open Project of Shanghai Key Laboratory of Veterinary Biotechnology (Grant no. klab201710).

## Compliance with ethical standards

**Conflict of interest** The authors declare that there are no conflicts of interests.

## References

- Song HZ, Qiang C, Xu DD, Yang X, Zheng XD (2016) Purified betacyanins from *Hylocereus undatus* peel ameliorate obesity and insulin resistance in high-fat-diet-fed mice. *J Agric Food Chem* 64:236–244
- Kopelman PG (2000) Obesity as a medical problem. *Nature* 404:635–643
- Williamson RM, Price JF, Glancy S, Perry E, Nee LD, Hayes PC, Frier BM, Van Look LA, Johnston GI, Reynolds RM (2011) Prevalence of and risk factors for hepatic steatosis and nonalcoholic fatty liver disease in people with type 2 diabetes: the edinburgh type 2 diabetes study. *Diabetes Care* 34:1139–1144
- Charytoniuk T, Drygalski K, Konstantynowicz-Nowicka K, Berk K, Chabowski A (2017) Alternative treatment methods attenuate the development of NAFLD: a review of resveratrol molecular mechanisms and clinical trials. *Nutrition* 34:108–117
- He HJ, Wang GY, Gao Y, Ling WH, Yu ZW, Jin TR (2012) Curcumin attenuates Nrf2 signaling defect, oxidative stress in muscle and glucose intolerance in high fat diet-fed mice. *World J Diabetes* 3:94–104
- Lin ZH, Cai FF, Lin N, Ye JI, Zheng QQ, Ding GS (2014) Effects of glutamine on oxidative stress and nuclear factor- $\kappa$ B expression in the livers of rats with nonalcoholic fatty liver disease. *Exp Ther Med* 7:365–370
- Allen L, Ramalingam L, Menikdiwela K, Scoggin S, Shen CL, Tomison MD, Kaur G, Dufour JM, Chung E, Kalupahana NS, Moustaid-Moussa N (2017) Effects of delta-tocotrienol on obesity-related adipocyte hypertrophy, inflammation and hepatic steatosis in high-fat-fed mice. *J Nutr Biochem* 48:128–137
- Musso G, Gambino R, Cassader M (2009) Recent insights into hepatic lipid metabolism in non-alcoholic fatty liver disease (NAFLD). *Prog Lipid Res* 48:1–26
- Tilg H, Moschen AR (2010) Evolution of inflammation in nonalcoholic fatty liver disease: the multiple parallel hits hypothesis. *Hepatology* 52:1836–1846
- Wang S, Zhu MJ, Du M (2014) Prevention of obesity by dietary resveratrol: how strong is the evidence? *Expert Rev Endocrinol Metab* 10:561–564
- Tian Y, Ma J, Wang W, Zhang L, Xu J, Wang K, Li D (2016) Resveratrol supplement inhibited the NF- $\kappa$ B inflammation pathway through activating AMPK $\alpha$ -SIRT1 pathway in mice with fatty liver. *Mol Cell Biochem* 422:75–84
- Labbé A, Garand C, Cogger VC, Paquet ER, Desbiens M, Le CD, Lebel M (2011) Resveratrol improves insulin resistance hyperglycemia and hepatosteatosis but not hypertriglyceridemia, inflammation, and life span in a mouse model for Werner syndrome. *J Gerontol A Biol Sci Med Sci* 66:264–278
- Shakibaei M, Harikumar KB, Aggarwal BB (2009) Resveratrol addiction: to die or not to die. *Mol Nutr Food Res* 53:115–128
- Delmas D, Lançon A, Colin D, Jannin B, Latruffe N (2006) Resveratrol as a chemopreventive agent: a promising molecule for fighting cancer. *Curr Drug Targets* 7:423–442
- Heebøll S, Thomsen KL, Pedersen SB, Vilstrup H, George J, Grønbaek H (2014) Effects of resveratrol in experimental and clinical non-alcoholic fatty liver disease. *World J Hepatol* 6:188–198
- Andrade JM, Paraíso AF, de Oliveira MV, Martins AM, Neto JF, Guimarães AL, de Paula AM, Qureshi M, Santos SH (2014) Resveratrol attenuates hepatic steatosis in high-fat fed mice by decreasing lipogenesis and inflammation. *Nutrition* 30:915–919
- Cho SJ, Jung UJ, Chol MS (2012) Differential effects of low-dose resveratrol on adiposity and hepatic steatosis in diet-induced obese mice. *Br J Nutr* 108:2166–2175
- Zhu W, Chen S, Li Z, Zhao X, Li W, Sun Y, Zhang Z, Ling W, Feng X (2014) Effects and mechanisms of resveratrol on the amelioration of oxidative stress and hepatic steatosis in KKAY mice. *Nutr Metab* 11:35
- Xu J, Zhang M, Zhang X, Yang H, Sun B, Wang Z, Zhou Y, Wang S, Liu X, Liu L (2018) Contribution of hepatic retinaldehyde dehydrogenase induction to impairment of glucose metabolism by high-fat diet feeding in C57BL/6J mice. *Basic Clin Pharmacol Toxicol* 123:539–548
- Li L, Hai J, Li Z, Zhang Y, Peng H, Li K, Weng X (2014) Resveratrol modulates autophagy and NF- $\kappa$ B activity in a murine model for treating non-alcoholic fatty liver disease. *Food Chem Toxicol* 63:166–173
- Ji G, Wang Y, Deng Y, Li X, Jiang Z (2015) Resveratrol ameliorates hepatic steatosis and inflammation in methionine/choline-deficient diet-induced steatohepatitis through regulating autophagy. *Lipids Health Dis* 14:134
- Matthews DR, Hosker JP, Rudenski AS, Naylor BA, Treacher DF, Turner RC (1985) Homeostasis model assessment: insulin resistance and  $\beta$ -cell function from fasting plasma glucose and insulin concentrations in man. *Diabetologia* 28:412–419
- Folch J, Lees M, Sloane Stanley GH (1957) A simple method for the isolation and purification of total lipids from animal tissues. *J Biol Chem* 226:497–509
- Bradford MM (1976) A rapid and sensitive method for the quantitation of microgram quantities of protein utilizing the principle of protein-dye binding. *Anal Biochem* 72:248–254
- Cheng K, Song ZH, Zheng XC, Zhang H, Zhang JF, Zhang LL, Zhou YM, Wang T (2017) Effects of dietary vitamin E type on the growth performance and antioxidant capacity in cyclophosphamide immunosuppressed broilers. *Poult Sci* 96:1159–1166
- Cheng K, Niu Y, Zheng XC, Zhang H, Chen YP, Zhang M, Huang XX, Zhang LL, Zhou YM, Wang T (2016) A comparison of natural (D- $\alpha$ -tocopherol) and synthetic (DL- $\alpha$ -tocopherol acetate) vitamin E supplementation on the growth performance, meat quality and oxidative status of broilers. *Asian-Australas J Anim Sci* 29:681–688
- Livak KJ, Schmittgen TD (2001) Analysis of relative gene expression data using real-time quantitative PCR and the 2<sup>- $\Delta\Delta$</sup> CT method. *Methods* 25:402–408
- Styskal JL, Remmen HV, Richardson A, Salmon AB (2012) Oxidative stress and diabetes: what can we learn about insulin

- resistance from antioxidant mutant mouse models? *Free Radic Biol Med* 52:46–58
29. Madan K, Bhardwaj P, Thareja S, Gupta SD, Saraya A (2006) Oxidant stress and antioxidant status among patients with non-alcoholic fatty liver disease (NAFLD). *J Clin Gastroenterol* 40:930–935
  30. Pan QR, Ren YL, Zhu JJ, Hu YJ, Zheng JS, Fan H, Xu Y, Wang G, Liu WX (2014) Resveratrol increases nephrin and podocin expression and alleviates renal damage in rats fed a high-fat diet. *Nutrients* 6:2619–2631
  31. Robb EL, Winkelmolen L, Visanji N, Brotchie J, Stuart JA (2008) Dietary resveratrol administration increases MnSOD expression and activity in mouse brain. *Biochem Biophys Res Commun* 372:254–259
  32. Truong VL, Jun M, Jeong WS (2018) Role of resveratrol in regulation of cellular defense systems against oxidative stress. *Biofactors* 44:36–49
  33. Jiang M, Li X, Yu X, Liu X, Xu X, He J, Gu H, Liu L (2017) Oral administration of resveratrol alleviates osteoarthritis pathology in C57BL/6J mice model induced by a high-fat diet. *Mediators Inflamm* 2017:7659023
  34. Yu S, Matsusue K, Kashireddy P, Cao WQ, Yeldandi V, Yeldandi AV, Rao MS, Gonzalez FJ, Reddy JK (2003) Adipocyte-specific gene expression and adipogenic steatosis in the mouse liver due to peroxisome proliferator-activated receptor gamma1 (PPAR-gamma1) overexpression. *J Biol Chem* 278:498–505
  35. Liu XJ, Wang BW, Zhang C, Xia MZ, Chen YH, Hu CQ, Wang H, Chen X, Xu DX (2015) Vitamin D deficiency attenuates high-fat diet-induced hyperinsulinemia and hepatic lipid accumulation in male mice. *Endocrinology* 156:2103–2113
  36. Koonen DP, Jacobs RL, Febbraio M, Young ME, Soltys CL, Ong H, Vance DE, Dyck JR (2007) Increased hepatic CD36 expression contributes to dyslipidemia associated with diet-induced obesity. *Diabetes* 56:2863–2871
  37. Luiken JJ, Dyck DJ, Han XX, Tandon NN, Arumugam Y, Glatz JF, Bonen A (2002) Insulin induces the translocation of the fatty acid transporter FAT/CD36 to the plasma membrane. *Am J Physiol Endocrinol Metab* 282:E491–E495
  38. Luiken JJ, Arumugam Y, Dyck DJ, Bell RC, Pelsers MM, Turcotte LP, Tandon NN, Glatz JF, Bonen A (2001) Increased rates of fatty acid uptake and plasmalemmal fatty acid transporters in obese Zucker rats. *J Biol Chem* 276:40567–40573
  39. Greco D, Kotronen A, Westerbacka J, Puig O, Arkkila P, Kiviluoto T, Laitinen S, Kolak M, Fisher RM, Hamsten A, Auvinen P, Yki-Jarvinen H (2008) Gene expression in human NAFLD. *Am J Physiol Gastrointest Liver Physiol* 294:G1281–G1287

**Publisher's Note** Springer Nature remains neutral with regard to jurisdictional claims in published maps and institutional affiliations.